Size and Shape-controlled Pd Nanocrystals on ZnO and SiO₂: When the Nature of the Support Determines the Active Phase

Micaela Crespo-Quesada,[a] Songhak Yoon,[b] Mingshang Jin,[c] Younan Xia,[d] Anke Weidenkaff,[b] and Lioubov Kiwi-Minsker[a]

Abstract: The structure sensitivity of acetylene hydrogenation was studied over size-controlled cubic and octahedral Pd nanocrystals supported on ZnO and SiO₂. Acetylene hydrogenation was found to be structure sensitive (with Pd(111) in octahedra being more active than Pd(100) in cubes). However, the response was found to vary depending on the redox properties of the support. The catalytically active and selective palladium carbide (PdC$_x$) phase was readily formed on the SiO₂-supported Pd NCs (much faster on cubes than on octahedra), while a markedly less active PdZn phase was preferentially formed on the ZnO-supported Pd nanocrystals. Here we show that the structure sensitivity of a chemical reaction is a complex phenomenon which originates from the reconstruction of the active phase in response to the reactive environment, which is ultimately determined by the support used.

Pd catalyzed alkyne hydrogenations are of special interest due to their importance in bulk and fine chemical production.[1] Acetylene hydrogenation is necessary to obtain polymer-grade ethylene, which tolerates extremely low quantities of the former (<5 ppm).[2] Acetylene hydrogenation has been identified as being *structure sensitive,*[3] *i.e.* that the catalytic behavior is influenced by the morphology (size and shape) of the Pd nanocrystals (NCs). Most studies deal with the effects of particle size,[4] and have found that the reaction shows antipathetic structure sensitivity, *i.e.* the TOF increases with increasing particle size.[3c, 5] The effects of shape, on the other hand, have been far less addressed. Although there are several theoretical studies of acetylene hydrogenation on single planes,[4, 6] there is only a handful of experimental results dealing with real catalysts, where the TOF was found to depend on the crystallographic plane exposed, showing activities Pd(111) > Pd(100),[5c] or correlating the catalytic response to the number of crystal boundaries present in a Pd nanowire.[7]

It is widely accepted that the performance of a catalyst in this reaction is governed by the changes in the Pd NCs imposed by the reacting molecules through the formation of hydride and carbide phases, which drastically impact on the observed catalytic behaviour with the PdC$_x$ being the active phase showing increased selectivity.[7-8] Furthermore, both experimental and theoretical[7, 8b, 9] studies have shown that PdC$_x$ formation is itself a structure sensitive phenomenon.[10] However, the behavior of supported Pd NCs can also be altered *via* interaction with the support induced by the physicochemical properties of the latter, *e.g.* acid-base and/or redox properties,[11] or by electronic interactions.[12] When a reducible oxide, such as ZnO, is used as a support, Zn atoms are incorporated into the Pd lattice forming a PdZn alloy phase. The presence of this phase was found to be beneficial in the hydrogenation of alkynols.[13] The formation of a PdZn phase imposes new adsorption properties, both towards hydrogen and the organic substrate, which, in turn, impact on the formation of the aforementioned palladium hydride and carbide species.

In this work, size-controlled Pd NCs of two shapes, *i.e.* cubes of 18 nm (CUB) of edge length and octahedra of 37 nm (OCT) of edge length were synthesized using Poly(vinyl)pyrrolidone (PVP) as stabilizing agent. The NCs were subsequently thoroughly cleaned-up from PVP, immobilized on commercial ZnO and SiO₂ and tested in the *semi*-hydrogenation of acetylene to assess the effect of the support on the evolution of the active phase during the reaction. Figure 1 shows transmission electron micrographs of the fresh catalysts while Table S1 in the Supporting Information gathers the main characteristics of the supported Pd NCs.

Multiple characterization techniques have demonstrated that the PdC$_x$ phase formed during acetylene hydrogenation retains the *fcc* structure of metallic Pd while C occupies the octahedral sites of the Pd lattice.[14] The incorporation of C atoms induces the expansion of the Pd lattice (increase of lattice parameter, *a*) in proportion to the fraction of guest atoms (x = C/Pd), as expressed by the following equation:[8j]

$$a = a_0 + 0.69x \ \text{(Å)} \tag{1}$$

We performed an *in situ* XRD analysis of all samples under reaction conditions (see Figure S1 in the Supporting Information) for determining the degree of carburization. The parameter x was obtained from the shift in the Bragg angle. Its change with time under catalytic reaction conditions, from metallic Pd (main reflection, Pd(111), 40.1°) to PdC$_x$ (39.1°), is shown in Figure 2a. The slope of such graph corresponds to

[a] Dr. M. Crespo-Quesada, Prof. L. Kiwi-Minsker
Group of Catalytic Reaction Engineering
Ecole Polytechnique Fédérale de Lausanne
Station 6, 1015 Lausanne (Switzerland)
E-mail: lioubov.kiwi-minsker@epfl.ch
[b] Dr. S. Yoon, Prof. A. Weidenkaff
Laboratory for Solid State Chemistry and Catalysis
Swiss Federal Laboratories for Materials Science and Technology
8600 Dübendorf (Switzerland)
[c] Prof. M. Jin
Metal Nanomaterials and Catalysis Research Group
Frontier Institute of Science and Technology
710054 Xi'an (China)
[d] Prof. Y. Xia
The Wallace H. Coulter Department of Biomedical Engineering
School of Chemistry and Biochemistry, and School of Chemical and Biomolecular Engineering
Georgia Institute of Technology
30332 Atlanta (USA)

Supporting information for this article is available on the WWW under http://dx.doi.org/10.1002/cctc.20xxxxxxx.

the Pd bulk carburization rate. In order to normalize the results per surface atom, the rates were divided by the actual Pd
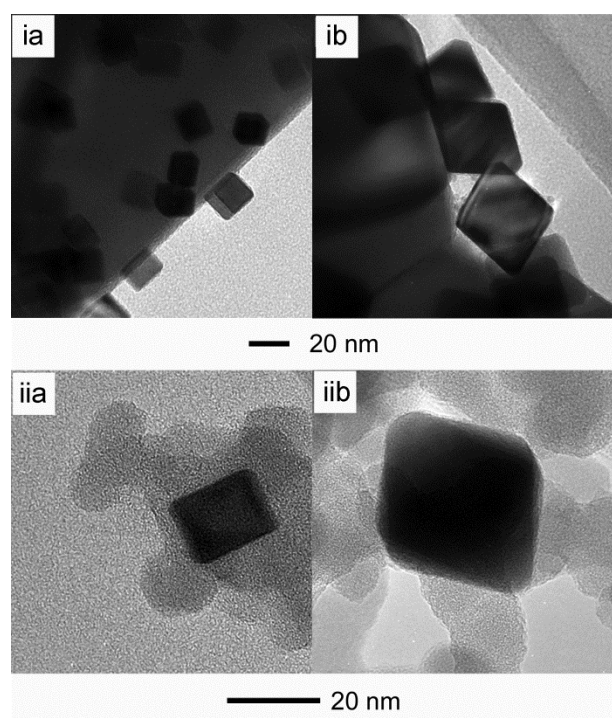

Figure 1. TEM pictures of i) ZnO supported and ii) SiO$_2$-supported Pd NCs: a) 18-nm cubes (CUB) and b) 37-nm octahedra (OCT).

dispersion for each catalyst (see Table S1 in the Supporting Information) and are presented in Figure 2b for CUB and OCT supported on both ZnO and SiO$_2$.

The carburization phenomenon was faster on the cubic Pd NCs on both supports, showing a ratio of $R_{C(CUB)}:R_{C(OCT)}$ equal to 3 on ZnO and 4 on SiO$_2$. This result confirms the preference of PdC$_x$ formation on Pd(100) with respect to Pd(111).[8e] NC size is important in structure-sensitive phenomena for sizes under 15 nm.[15] Since both NCs are larger than this limit, the difference in carburization rate can be attributed solely to shape effects (or crystallographic orientation). However, the surface carburization rate of ZnO-supported Pd NCs was found to be 10-fold lower than that of SiO$_2$-supported Pd NCs on fresh catalysts. In order to determine the reasons for this difference, the nature of the support must be taken into account. One of the most important characteristics influencing the catalytic performance is the support redox properties.[10] While SiO$_2$ is a non-reducible oxide, ZnO has been found to readily reduce under hydrogen in the presence of Pd NCs, thus creating an intermetallic PdZn phase.[13, 16] This phase imposes new adsorption properties on the catalyst, both towards hydrogen and the organic substrate. PdZn alloy formation was found to start already at around 373 K, likely from the surface, progressing into the bulk with increasing temperature, according to *in situ* high-resolution X-Ray diffraction (XRD) and X-Ray absorption spectroscopy (XAS).[17] In this particular case, Zn is believed to act both through an ensemble effect (especially at high Zn concentrations) by a "skin" model, rather than a progressive front of PdZn phase,[16c] and through an electronic effect, described as "long-range", which was found

to be strong enough to drastically modify the catalytic behavior of Pd in the presence of very small amounts of Zn by rearranging the electronic structure of the active metal.[18]

Therefore, we investigated the tendency of each ZnO-supported sample towards alloy formation through an *in situ* XRD analysis conjugated with temperature programmed reaction (TPR). Figure S2 in the Supporting Information shows
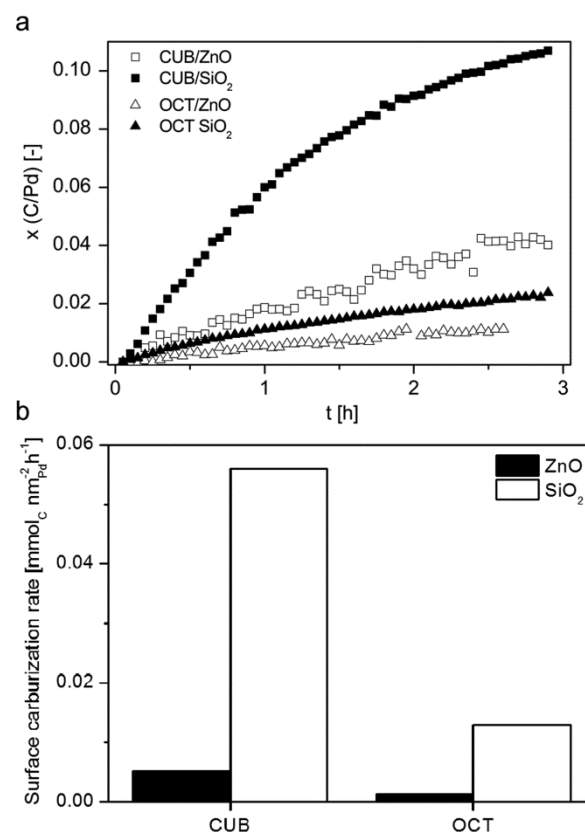

Figure 2. a) Time-resolved incorporation of C into the Pd lattice in terms of carburization degree and b) bulk carburization rate (obtained from panel a), and surface carburization rate of each catalyst. Conditions: 373 K, C$_2$H$_2$:H$_2$:N$_2$ = 2:4:94, 100 cm^3 min^{-1}.

the evolution in the main reflection of Pd NCs while heated up under a flow of 10% H$_2$/90% N$_2$.

The onset of the formation of PdZn for CUB/ZnO occurs at about 30 K lower temperature than for OCT/ZnO, suggesting a faster kinetics for alloy formation in the former. It is worth mentioning that these results, while confirming the structure sensitive nature of alloy formation, do not contradict the evidence showing its onset at temperatures as low as 373 K.[17] While those results were obtained with XAS, which is extremely sensitive to the environment of single Pd atoms, the XRD analysis is a bulk measurement, where considerable amounts of alloy must be formed before being detected. Moreover, it was performed at a relatively fast temperature ramp, thus shifting the alloy formation onset to higher temperatures. This allows proposing, judging by the results shown in Figure 2b, that the PdZn intermetallic phase formed on the ZnO support, significantly slowing down the formation of the active PdC$_x$ phase. A similar result had been found over Pd-Au catalysts in the synthesis of vinyl acetate,[19] and

suggests that site separation, rather than the nature of the alloying metal, is responsible for the decreased substrate adsorption and C-C bond scission, with the subsequent incorporation of C in the Pd lattice.

The results shown above imply that the nature of the active phase of the catalysts under reaction conditions is drastically modified by the reacting molecules and the support. In both cases, this modification was found to be structure sensitive,
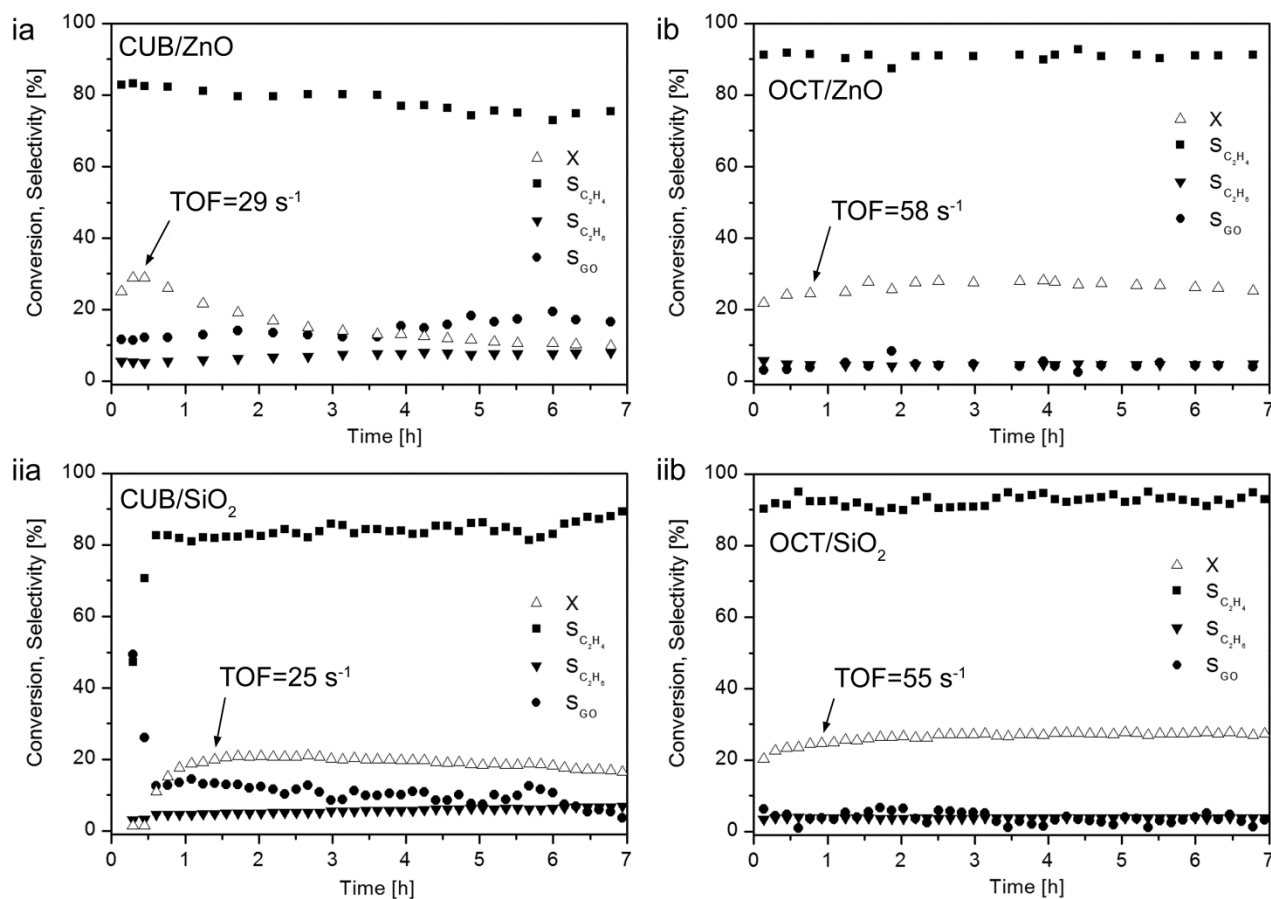

Figure 3. Acetylene conversion (X) and selectivity (S_i) towards ethylene, ethane and green oil (GO) with time on stream for i) ZnO-supported and ii) SiO$_2$-supported a) CUB and b) OCT catalysts, respectively. Reaction conditions: 373 K, C$_2$H$_2$:H$_2$:Ar = 2:4:94, 800 cm^3 min^{-1}.

with cubic Pd NCs being modified much faster than octahedra, probably due to the more open arrangement of the atoms on the surface. However, when ZnO is used as carrier, the formation of PdZn was found to form preferentially compared to the PdC$_x$ phase. Therefore, SiO$_2$-supported catalysts showed a PdC$_x$ phase under steady-state, whereas ZnO-supported catalysts showed a PdZn rich phase, with little to no PdC$_x$ on their surfaces.

The catalysts were subsequently tested in the hydrogenation of acetylene as a probe reaction to assess the catalytic performance of each type of active phase. Figure 3 shows the conversion and selectivity on time corresponding to a 7 h run for all samples.

The first clear difference arises at the very beginning of the reaction for CUB catalysts showing an induction period, which can be correlated to the high carburization rate on this catalyst. Probably, the first molecules of acetylene getting in contact with bare Pd(100) are strongly adsorbed and hence readily decomposed to C atoms, outright able to diffuse into the metallic lattice. A similar conclusion was drawn from recent DFT calculations on several different surfaces of Pd.[20] After a critical amount of C has been incorporated to the Pd(100)

lattice, the interaction weakens and acetylene begins to be hydrogenated. On the other hand, CUB/ZnO catalyst shows a significant activity towards acetylene hydrogenation from the reaction onset (TOF=29 s^{-1}), suggesting that the migration of Zn starts to occur already at the very beginning of the reaction, thus changing the adsorption properties of acetylene, which can in this case be hydrogenated instead of being transformed into PdC$_x$. Indeed, this value is roughly the same as the activity on CUB/SiO$_2$ once carbon has started to diffuse into the nanoparticles (25 s^{-1}). This finding is in line with a recent work showing that the addition of foreign atoms into the Pd lattice has the similar effects regardless of the nature of the guest atoms.[8a] Furthermore, while the selectivity towards ethylene is comparable on both catalysts, CUB/ZnO suffers a marked deactivation starting from low reaction times, whereas CUB/SiO$_2$ deactivates slowly, probably due to the accumulation of green oil on the catalyst. This suggests that the continued formation of PdZn on the former decreases the activity towards acetylene hydrogenation, in line with results obtained on acetylenic alcohols.[13, 21] The different reactivity of the PdZn and PdC$_x$ phases can be rationalized from the viewpoint of the lattice parameter distortion exerted by the

addition of interstitial C (2.3% increase in a), or by the incorporation of Zn in the Pd lattice (2.3% decrease in a), which can be estimated from the Bragg angle shifts observed experimentally. Furthermore, in the case of PdZn, the incorporated Zn atoms "dilute" the Pd adsorption sites.

As far as OCT catalysts are concerned, a similar selectivity and activity is found at the beginning of the reaction. This underlines the structure sensitive nature of both PdZn and PdC_x formation, which are greatly hindered on Pd(111). However, while OCT/SiO_2 catalyst is remarkably stable with time, OCT/ZnO starts to deactivate after about 4 h on stream. In order to study this phenomenon in detail, 14 h runs for the ZnO-supported catalysts were performed and are shown in Figure S3. It can be indeed seen that OCT/SiO_2 maintains its activity during a 14 h run, while OCT/ZnO deactivates by 37%. In all cases, OCT samples were more active than the cubic counterparts, in line with other works on the literature presenting Pd(111) as more active than Pd(100).[5c] This probably arises from the difference in adsorption energy on both surfaces. While the interaction of acetylene with Pd(100) is stronger than with Pd(111),[20] the reaction order is reported to be negative,[22] and therefore, lower heat of adsorptions would lead to increased reaction rates.

In conclusion, the structure sensitivity of acetylene hydrogenation was studied over size-controlled cubic and octahedral Pd NCs supported on ZnO and SiO_2. Critical modification of Pd NCs was observed by $in\ situ$ XRD under technologically relevant reaction conditions. While acetylene hydrogenation is indeed structure sensitive (with Pd(111) in octahedra being more active than Pd(100) in cubes), the response was found to vary depending on the redox properties of the support. The catalytically active and selective palladium carbide (PdC_x) phase was readily formed on the SiO_2-supported Pd NCs (much faster on cubes than on octahedra), while a markedly less active PdZn phase was preferentially formed on the ZnO-supported Pd NCs, which, in turn, significantly slowed down the formation of PdC_x. Therefore, we present herein direct evidence that the structure sensitivity of a chemical reaction (acetylene hydrogenation as a case study) is a complex phenomenon which originates from the intrinsic structure sensitivity of the reconstruction of Pd NCs in response to the reactive environment which is controlled by the support used.

Experimental Section

Preparation of the nanocrystals. The Pd nanocubes were synthesized according to our previously published protocols.[23] In a typical synthesis, 11 mL of an aqueous solution containing poly(vinyl pyrrolidone) (PVP, MW ≈ 55,000, 105 mg, Aldrich), L-ascorbic acid (60 mg, Aldrich), KBr (600 mg, Fisher), and sodium tetrachloropalladate (Na_2PdCl_4, 57 mg, Aldrich) were heated at 353 K in air under magnetic stirring for 3 h. The Pd octahedra were prepared as reported in our previous protocol.[24] In a typical procedure, 3 mL of aqueous Na_2PdCl_4 solution (32 mM) was introduced into 8 mL of an aqueous solution containing 105 mg PVP, 100 μL HCHO, and 0.3 mL of an aqueous suspension (1.8 mg/mL in concentration) of Pd cubic seeds 18 nm in edge length, which had been heated at 333 K for 5 min under magnetic stirring in a capped vial. The reaction was then allowed to proceed at 333 K for 3 h. The final products were collected by centrifugation and washed with

ethanol and water to remove excess PVP. The NCs were subsequently immobilized on commercially available SiO_2 (S5505, Sigma-Aldrich) and ZnO (44263, Alfa Aesar) by wet impregnation.

Characterization techniques. The shape and size of the Pd NCs were analysed by transmission electron microscopy (TEM), using a Philips CM12 microscope operated at 120 kV.

To determine the amount of Pd in each catalyst, an aliquot of the nanoparticle suspension was analysed by atomic absorption spectroscopy (AAS, Shimadzu AA-6650). The specific wavelength used for Pd^{2+} was 475 nm.

$In\ situ$ powder XRD patterns were obtained using a PANalytical X´Pert PRO θ-θ scan system with Cu-K_α radiation (λ = 1.5418 Å). The diffraction patterns were recorded with an angular step of 0.05˚. The powder samples were placed in the heating chamber (XRK 900, Anton Paar) and gas was applied through the mass flow controller (5850 TR, Brooks instrument). The used gas were N_2 (99.999%, Messer), H_2 (99.999%, Messer and C_2H_2 (> 99.5%, PanGas). Roughly 0.03 g of sample powders was heated under N_2 flow (cm^3 min^{-1}) up to 373 K or 423 K with a heating rate of 10 K min^{-1}. Peak fitting was performed using the software $Fityk$.[25]

Active metal dispersion and surface area were determined through CO chemisorption using Micromeritics (Autochem II 2920). The samples were loaded into a U-shaped quartz cell (3.76 mm i.d.), heated in 20 cm^3 min^{-1} 2% H_2/He at 10 K min^{-1} to 373 K and held for 15 min. The samples were subsequently out gassed in Ar at 373 K for 30 min after which the temperature was decreased to ambient conditions. The CO-chemisorption experiments were performed at 323 K using He as carrier gas. A 3% CO/He mixture gas was pulsed through the sample until the peaks were equal. In a series of blank tests, chemisorption measurements on SiO_2 did not result in any detectable uptake.

Acetylene hydrogenation. The reaction was carried out in a stainless steel tubular reactor with an inner diameter of 12 mm. The powdered catalyst was introduced in the reactor between two layers of glass wool and secured by means of a hollow shaft. In order to ensure a uniform flow distribution, the reactor was filled up with glass beads. 800 cm^3 min^{-1} of a 2% C_2H_2/4% H_2/Ar mixture was flown through the reactor bed at 373 K for several hours. A pressure of 104 kPa was maintained during the reaction. The concentration of products was followed by GC using an HP 6890 gas chromatograph (Agilent Technology AG) equipped with a Carboxen 1010 capillary column (Fluka Holding AG).

[1] H. U. Blaser, $Catal.\ Today$ **2000**, 60, 161-165.
[2] D. H. Mei, M. Neurock, C. M. Smith, $J.\ Catal.$ **2009**, 268, 181-195.
[3] a) A. Borodziński, $Catal.\ Lett.$ **2001**, 71, 169-175; b) M. Ruta, G. Laurenczy, P. J. Dyson, L. Kiwi-Minsker, $J.\ Phys.\ Chem.\ C$ **2008**, 112,

17814-17819; c) P. Tribolet, L. Kiwi-Minsker, *Catal. Today* **2005**, *105*, 337-343.

[4] D. Duca, Z. Varga, G. La Manna, T. Vidoczy, *Theor. Chem. Acc.* **2000**, *104*, 302-311.

[5] a) M. Che, C. O. Bennett, *Adv. Catal.* **1989**, *36*, 55-172; b) M. Ruta, N. Semagina, L. Kiwi-Minsker, *J. Phys. Chem. C* **2008**, *112*, 13635-13641; c) A. E. Yarulin, R. M. Crespo-Quesada, E. V. Egorova, L. L. K. Minsker, *Kinet. Catal.* **2012**, *53*, 253-261.

[6] D. Duca, G. Barone, Z. Varga, *Catal. Lett.* **2001**, *72*, 17-23.

[7] Y. F. He, J. T. Feng, Y. Y. Du, D. Q. Li, *ACS Catal.* **2012**, *2*, 1703-1710.

[8] a) M. Armbrüster, M. Behrens, F. Cinquini, K. Föttinger, A. Grin, A. Haghofer, B. Klötzer, A. Knop-Gericke, H. Lorenz, A. Ota, S. Penner, J. Prinz, C. Rameshan, Z. Révay, D. Rosenthal, G. Rupprechter, P. Sautet, R. Schlögl, L. Shao, L. Szentmiklósi, D. Teschner, D. Torres, R. Wagner, R. Widmer, G. Wowsnick, *ChemCatChem* **2012**, *4*, 1048-1063; b) N. Seriani, F. Mittendorfer, G. Kresse, *J. Chem. Phys* **2010**, *132*; c) D. Teschner, J. Borsodi, A. Wootsch, Z. Révay, M. Hävecker, A. Knop-Gericke, S. D. Jackson, R. Schlögl, *Science* **2008**, *320*, 86-89; d) D. Teschner, Z. Revay, J. Borsodi, M. Havecker, A. Knop-Gericke, R. Schlogl, D. Milroy, S. D. Jackson, D. Torres, P. Sautet, *Angew. Chem. Int. Edit.* **2008**, *47*, 9274-9278; e) D. Teschner, E. Vass, M. Havecker, S. Zafeiratos, P. Schnorch, H. Sauer, A. Knop-Gericke, R. Schloegl, M. Chamam, A. Wootsch, A. S. Canning, J. J. Gamman, S. D. Jackson, J. McGregor, L. F. Gladden, *J. Catal.* **2006**, *242*, 26-37; f) M. W. Tew, M. Janousch, T. Huthwelker, J. A. van Bokhoven, *J. Catal.* **2011**, *283*, 45-54; g) M. W. Tew, J. T. Miller, J. A. van Bokhoven, *J. Phys. Chem. C* **2009**, *113*, 15140-15147; h) M. W. Tew, M. Nachtegaal, M. Janousch, T. Huthwelker, J. A. van Bokhoven, *Phys. Chem. Chem. Phys.* **2012**, *14*, 5761-5768; i) E. M. Vass, M. Havecker, S. Zafeiratos, D. Teschner, A. Knop-Gericke, R. Schlogl, *J. Phys.-Condens. Mat.* **2008**, *20*; j) W. Vogel, *J. Phys. Chem. C* **2011**, *115*, 1506-1512.

[9] A. M. Doyle, S. K. Shaikhutdinov, S. D. Jackson, H. J. Freund, *Angew. Chem. Int. Edit.* **2003**, *42*, 5240-5243.

[10] M. Crespo-Quesada, F. Cárdenas-Lizana, A.-L. Dessimoz, L. Kiwi-Minsker, *ACS Catal.* **2012**, *2*, 1773-1786.

[11] a) H. Bonnemann, W. Brijoux, K. Siepen, J. Hormes, R. Franke, J. Pollmann, J. Rothe, *App. Organomet. Chem.* **1997**, *11*, 783-796; b) N. A. Zakarina, G. D. Zakumbaeva, N. F. Toktabaeva, B. B. Dyusenbina, E. N. Litvyakova, A. S. Kuanyshev, *Kinet. Catal.* **1983**, *24*, 733-737.

[12] a) C. Park, M. A. Keane, *J. Colloid. Interf. Sci.* **2003**, *266*, 183-194; b) M. L. Toebes, Y. H. Zhang, J. Hajek, T. A. Nijhuis, J. H. Bitter, A. J. van Dillen, D. Y. Murzin, D. C. Koningsberger, K. P. de Jong, *J. Catal.* **2004**, *226*, 215-225.

[13] M. Crespo-Quesada, M. Grasemann, N. Semagina, A. Renken, L. Kiwi-Minsker, *Catal. Today* **2009**, *147*, 247-254.

[14] a) J. A. Mccaulley, *J. Phys. Chem.* **1993**, *97*, 10372-10379; b) S. B. Ziemecki, G. A. Jones, D. G. Swartzfager, R. L. Harlow, *J. Am. Chem. Soc.* **1985**, *107*, 4547-4548.

[15] M. Crespo-Quesada, A. Yarulin, M. S. Jin, Y. N. Xia, L. Kiwi-Minsker, *J. Am. Chem. Soc.* **2011**, *133*, 12787-12794.

[16] a) N. Iwasa, S. Masuda, N. Ogawa, N. Takezawa, *Appl. Catal. A* **1995**, *125*, 145-157; b) M. G. Musolino, C. Busacca, F. Mauriello, R. Pietropaolo, *Appl. Catal. A* **2010**, *379*, 77-86; c) A. Sarkany, Z. Zsoldos, B. Furlong, J. W. Hightower, L. Guczi, *J. Catal.* **1993**, *141*, 566-582; d) N. Semagina, M. Grasemann, N. Xanthopoulos, A. Renken, L. Kiwi-Minsker, *J. Catal.* **2007**, *251*, 213-222; e) P. S. Wehner, G. C. Tustin, B. L. Gustafson, *J. Catal.* **1984**, *88*, 246 - 248; f) Z. Zsoldos, A. Sarkany, L. Guczi, *J. Catal.* **1994**, *145*, 235-238.

[17] M. W. Tew, H. Emerich, J. A. van Bokhoven, *J. Phys. Chem. C* **2011**, *115*, 8457-8465.

[18] a) E. Jeroro, M. P. Hyman, J. M. Vohs, *Phys. Chem. Chem. Phys.* **2009**, *11*, 10457-10465; b) E. Jeroro, J. M. Vohs, *J. Phys. Chem. C* **2009**, *113*, 1486-1494; c) E. Jeroro, J. M. Vohs, *Catal. Lett.* **2009**, *130*, 271-277.

[19] Y. F. Han, D. Kumar, C. Sivadinarayana, A. Clearfield, D. W. Goodman, *Catal. Lett.* **2004**, *94*, 131-134.

[20] B. Yang, R. Burch, C. Hardacre, G. Headdock, P. Hu, *J. Catal.* **2013**, *305*, 264-276.

[21] N. Semagina, A. Renken, D. Laub, L. Kiwi-Minsker, *J. Catal.* **2007**, *246*, 308-314.

[22] A. Borodziński, G. C. Bond, *Catal. Rev.-Sci. Eng.* **2008**, *50*, 379-469.

[23] a) M. Jin, H. Liu, H. Zhang, Z. Xie, J. Liu, Y. Xia, *Nano Res.* **2011**, *4*, 83-91; b) B. Lim, M. J. Jiang, J. Tao, P. H. C. Camargo, Y. M. Zhu, Y. N. Xia, *Adv. Funct. Mater.* **2009**, *19*, 189-200.

[24] M. S. Jin, H. Zhang, Z. X. Xie, Y. N. Xia, *Energ. Environ. Sci.* **2012**, *5*, 6352-6357.

[25] M. Wojdyr, *J. Appl. Crystallogr.* **2010**, *43*, 1126-1128.

Entry for the Table of Contents

COMMUNICATION

The structure sensitivity of Pd-catalyzed acetylene hydrogenation is the consequence of the profound rearrangements occurring within Pd NCs in response to the reactive environment and is controlled by the support. Active PdCx was formed on SiO2, while Pd NCs supported on ZnO preferentially formed PdZn, rendering a less active and unstable catalyst.
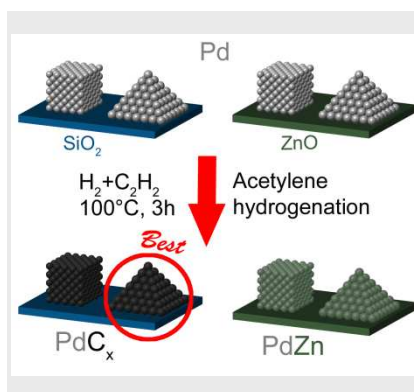
Micaela Crespo-Quesada, Songhak Yoon, Mingshang Jin, Younan Xia, Anke Weidenkaff and Lioubov Kiwi-Minsker*

Size and shape-controlled Pd nanocrystals on ZnO and SiO$_2$: when the nature of the support determines the active phase